

ORIGINAL ARTICLE

Airway “Resistotypes” and Clinical Outcomes in Bronchiectasis

✉ Micheál Mac Aogáin^{1,2,3*}, Fransiskus Xaverius Ivan^{3*}, Tavleen Kaur Jaggi³, Hollian Richardson⁴, Amelia Shoemark⁴, Jayanth Kumar Narayana³, Alison J. Dicker⁴, Mariko Siyue Koh⁵, Ken Cheah Hooi Lee⁵, Ong Thun How⁵, Mau Ern Poh⁶, Ka Kiat Chin⁶, Albert Lim Yick Hou^{3,7}, Puah Ser Hon^{3,7}, Teck Boon Low⁸, John Arputhan Abisheganaden^{3,7}, Katerina Dimakou⁹, Antonia Digalaki⁹, Chrysavgi Kosti⁹, Anna Gkousiou⁹, Philip M. Hansbro¹⁰, Francesco Blasi^{11,12}, Stefano Aliberti^{13,14}, James D. Chalmers⁴, and Sanjay H. Chotirmall^{3,7}

¹Biochemical Genetics Laboratory, Department of Biochemistry, St. James's Hospital, Dublin, Ireland; ²Clinical Biochemistry Unit, School of Medicine, Trinity College Dublin, Dublin, Ireland; ³Lee Kong Chian School of Medicine, Nanyang Technological University, Singapore; ⁴University of Dundee, Ninewells Hospital and Medical School, Dundee, United Kingdom; ⁵Department of Respiratory and Critical Care Medicine, Singapore General Hospital, Singapore; ⁶Department of Medicine, Faculty of Medicine, Universiti Malaya, Kuala Lumpur, Malaysia; ⁷Department of Respiratory and Critical Care Medicine, Tan Tock Seng Hospital, Singapore; ⁸Department of Respiratory and Critical Care Medicine, Changi General Hospital, Singapore; ⁹5th Respiratory Medicine Department, General Hospital for Chest Diseases of Athens “Sotiria”, Athens, Greece; ¹⁰Centre for Inflammation, Centenary Institute and University of Technology Sydney, Faculty of Science, School of Life Sciences, Sydney, Australia; ¹¹Respiratory Unit and Cystic Fibrosis Center, Foundation IRCCS Ca' Granda Ospedale Maggiore Policlinico, Milan, Italy; ¹²Department of Pathophysiology and Transplantation, University of Milan, Milan, Italy; ¹³Department of Biomedical Sciences, Humanitas University, Milan, Italy; and ¹⁴IRCCS Humanitas Research Hospital, Respiratory Unit, Rozzano, Milan, Italy

ORCID IDs: 0000-0002-1726-7700 (M.M.A.); 0000-0001-7360-6060 (A.S.); 0000-0003-0417-7607 (S.H.C.).

Abstract

Rationale: Chronic infection and inflammation shapes the airway microbiome in bronchiectasis. Utilizing whole-genome shotgun metagenomics to analyze the airway resistome provides insight into interplay between microbes, resistance genes, and clinical outcomes.

Objectives: To apply whole-genome shotgun metagenomics to the airway microbiome in bronchiectasis to highlight a diverse pool of antimicrobial resistance genes: the “resistome,” the clinical significance of which remains unclear.

Methods: Individuals with bronchiectasis were prospectively recruited into cross-sectional and longitudinal cohorts ($n = 280$), including the international multicenter cross-sectional Cohort of Asian and Matched European Bronchiectasis 2 (CAMEB 2) study ($n = 251$) and two independent cohorts, one describing patients experiencing acute exacerbation and a further cohort of patients undergoing *Pseudomonas aeruginosa* eradication treatment. Sputum was subjected to metagenomic sequencing, and the bronchiectasis resistome was evaluated in association with clinical outcomes and underlying host microbiomes.

Measurements and Main Results: The bronchiectasis resistome features a unique resistance gene profile and increased

counts of aminoglycoside, bicyclomycin, phenicol, triclosan, and multidrug resistance genes. Longitudinally, it exhibits within-patient stability over time and during exacerbations despite between-patient heterogeneity. Proportional differences in baseline resistome profiles, including increased macrolide and multidrug resistance genes, associate with shorter intervals to the next exacerbation, whereas distinct resistome archetypes associate with frequent exacerbations, poorer lung function, geographic origin, and the host microbiome. Unsupervised analysis of resistome profiles identified two clinically relevant “resistotypes,” RT1 and RT2, the latter characterized by poor clinical outcomes, increased multidrug resistance, and *P. aeruginosa*. Successful targeted eradication in *P. aeruginosa*-colonized individuals mediated reversion from RT2 to RT1, a more clinically favorable resistome profile demonstrating reduced resistance gene diversity.

Conclusions: The bronchiectasis resistome associates with clinical outcomes, geographic origin, and the underlying host microbiome. Bronchiectasis resistotypes link to clinical disease and are modifiable through targeted antimicrobial therapy.

Keywords: bronchiectasis; microbiome; metagenomics; resistome; resistotype

(Received in original form June 19, 2023; accepted in final form January 16, 2024)

✉ This article is open access and distributed under the terms of the Creative Commons Attribution Non-Commercial No Derivatives License 4.0. For commercial usage and reprints, please e-mail Diane Gern (dgern@thoracic.org).

*These authors contributed equally to this work.

This article has a related editorial.

Am J Respir Crit Care Med Vol 210, Iss 1, pp 47–62, Jul 1, 2024

Copyright © 2024 by the American Thoracic Society

Originally Published in Press as DOI: 10.1164/rccm.202306-1059OC on January 25, 2024

Internet address: www.atsjournals.org

At a Glance Commentary

Scientific Knowledge on the

Subject: The microbiome in bronchiectasis demonstrates geographic variability, correlates clinically with disease progression and outcomes, and incorporates a distinct repertoire of antimicrobial resistance genes known as the resistome. The clinical and therapeutic implications of the resistome in bronchiectasis remain unclear.

What This Study Adds to the

Field: We present the largest study of the bronchiectasis resistome to date, including patients from five countries in clinically “matched” cohorts of Asian and European origin. We demonstrate the relevance of the resistome to clinical outcomes in bronchiectasis and outline novel “resistotypes” with therapeutic implications. Targeted eradication of specific airway microbes that exhibit broad resistance gene profiles mediates reversion to more clinically favorable resistotypes, suggesting that bronchiectasis resistomes can be modified for therapeutic benefit.

functional capabilities of its constituent microbial taxa, including the expression of antimicrobial resistance (AMR) (3, 4).

Antibiotic agent use in bronchiectasis, although important, has lacked the anticipated impact for this “infective” condition, suggesting a more complex, dynamic, and evolving understanding of pathogenesis, advanced by the “vicious vortex” hypothesis (1). Mechanisms through which antibiotic agents function in bronchiectasis, going beyond microbial killing, remain unclear, reflected by the repeated failure of several multicenter antibiotic-focused clinical trials (5–9). The consideration of other influences such as geographic heterogeneity, airway inflammation, and underlying AMR will allow an improved understanding of antibiotic therapy in bronchiectasis, leading to better clinical success (10–12). Current clinical practice relies heavily on the detection of dominant culturable pathogens, which presents a limited perspective (2, 13).

The airway microbiome, characterized by diverse AMR genes (ARGs), exhibits variability across chronic respiratory disease states, including bronchiectasis (10, 14–16). Innovations in sequencing technologies and bioinformatics have accelerated the functional appraisal of the microbiome, including its resistome (4, 10). The chronicity of bronchiectasis, coupled with its repeated cycles of recurrent infection and antimicrobial therapy, likely have important implications on the airway resistome: one that defines the survival and colonization capabilities of individual microorganisms within a host microbiome. Higher levels of AMR favor overgrowth of drug-resistant microorganisms, potentially shaping

microbiome composition, function, and disease outcome (14–16). Following antibiotic treatment, microbial alteration ensues, leading to changes in microbial burden, gene expression, and/or metabolite production (17, 18).

Despite established links between the bronchiectasis microbiome and clinical outcomes, the role and influence of the resistome remain unclear. Here, we report the largest study of the bronchiectasis resistome to date, encompassing cross-sectional and longitudinally sampled cohorts. We present assessment of patients in stable condition from five countries in clinically “matched” cohorts of Asian and European origin, allowing the assessment of clinical association with respect to geographic variability while carefully assessing resistome stability in response to alternative antimicrobial treatment regimens in serially sampled subjects. We describe the clinical correlates of the resistome and outline novel “resistotypes” with therapeutic implications. Some of the results of these studies have been previously reported in abstract form (19–21).

Methods

Study Populations

The study was designed to investigate the variability of the resistome and its clinical implications in bronchiectasis. To this end, four clinical cohorts were recruited to this study, each receiving appropriate ethical approval (*see* online supplement). All recruited individuals provided written informed consent for participation. The four cohorts are summarized as follows.

Emerging work on the lung microbiome underscores its centrality to infection, inflammation, and disease progression in bronchiectasis (1, 2). Principal to this are the

Supported by the Singapore Ministry of Health's National Medical Research Council under Clinician-Scientist Individual Research Grants MOH-000141 and MOH-001356 (S.H.C.) and Clinician-Scientist Award MOH-000710 (S.H.C); the Singapore Ministry of Education under its AcRF Tier 1 Grant (RT1/22) (S.H.C); a fellowship and grant from the National Health and Medical Research Council of Australia (1059238, 1175134, and 2010287; P.M.H.); Ministero della Salute, Ricerca Corrente Fondazione IRCCS Ca' Granda Ospedale Maggiore Policlinico 260/01/2022; and European Multicentre Bronchiectasis Audit and Research Collaboration (EMBARC) 3, which is funded by the European Respiratory Society through the EMBARC3 clinical research collaboration.

Author Contributions: M.M.A.: experimental design, data analysis and visualization, oversight of bioinformatic and statistical codebase, writing the manuscript. F.X.I.: oversight of computation and metagenomic data engineering, bioinformatic and statistical analysis, data visualization, writing the manuscript. T.K.J. and H.R.: management and curation of clinical samples and data, sample preparation, DNA extraction, amplification, and sequencing. J.K.N.: data analysis and interpretation. A.S., A.J.D., M.S.K., K.C.H.L., O.T.H., M.E.P., K.K.C., A.L.Y.H., P.S.H., T.B.L., J.A.A., K.D., A.D., C.K., A.G., F.B., and S.A.: patient recruitment, clinical data and specimen collection, intellectual contribution. P.M.H.: intellectual contribution. J.D.C.: conception and design of experiments, recruitment of patients, and procurement of clinical data and specimens. S.H.C.: conception and design of overall study and experiments, data analysis and interpretation, statistical analysis, writing the manuscript, and procurement of funding.

Correspondence and requests for reprints should be addressed to Sanjay H. Chotirmall, M.D., Ph.D., Lee Kong Chian School of Medicine, Nanyang Technological University, 11 Mandalay Road, Singapore 308232. E-mail: schotirmall@ntu.edu.sg.

A data supplement for this article is available via the Supplements tab at the top of the online article.

The first cohort was the nondiseased (comparator) cohort: to provide a baseline comparator of the “healthy” resistome in nondiseased individuals for reference, 25 never-smoking individuals with no history of respiratory or other known medical diseases and with normal spirometry were recruited in Singapore, with clinical data obtained and (induced) sputum sampling performed.

The second cohort was the cross-sectional Cohort of Asian and Matched European Bronchiectasis 2 (CAMEB 2): to comprehensively assess the variability and clinical correlates of the airway resistome in bronchiectasis, 251 patients with bronchiectasis (confirmed in accordance with British Thoracic Society guidelines [22]) were prospectively recruited across four countries (Singapore, Malaysia, Scotland [United Kingdom], and Italy), forming part of the cross-sectional CAMEB 2 study, a follow-up cohort from the original CAMEB study (23). Here, 130 individuals with stable bronchiectasis were recruited, with complete clinical data collation and sputum sampling, across four Asian sites: three in Singapore (Singapore General Hospital, Changi General Hospital, and Tan Tock Seng Hospital) and one in Malaysia (University of Malaya Medical Centre), a subset of which ($n = 97$) were matched based on age, sex, exacerbation frequency, and lung function (as FEV₁% predicted) to a European cohort ($n = 112$) recruited at two sites: one in Scotland (Ninewells Hospital, Dundee, United Kingdom) and one in Italy (Fondazione Istituto di Ricovero e Cura a Carattere Scientifico Ca' Granda Ospedale Maggiore Policlinico, Milan, Italy) (Table 1). Patients were recruited during periods of clinical stability, defined by the absence of new symptoms and/or change in bronchiectasis therapy with no exacerbations and/or acute antibiotic treatment in the preceding 4-week period. Exclusion criteria included other concurrent major respiratory diagnoses, including asthma or chronic obstructive pulmonary disease, as established by international criteria including spirometry (24, 25). Individuals receiving chemotherapy and those with acute and/or recent infection requiring short-term antibiotic therapy (oral or intravenous) in the 4 weeks preceding outpatient attendance were excluded.

The third cohort was the bronchiectasis exacerbation cohort. To assess the stability of the airway resistome over time and in response to acute antimicrobial treatment, two independent bronchiectasis cohorts were

recruited: one in Singapore that was followed during clinical stability for 3–7 months with repeated sputum sampling and a second from two sites in the east of Scotland ($n = 18$) who had undergone sampling before, during, and after exacerbations. For the latter cohort, patients were enrolled during periods of clinical stability and asked to provide a spontaneous sputum sample at baseline (preexacerbation sample) and then followed closely, with repeat sputum sampling performed ≤ 24 hours after commencing antibiotic therapy (exacerbation sample) and then after 14 days of antibiotic treatment (postexacerbation sample). The final postexacerbation sample was obtained after cessation of antibiotic therapy on day 14 when clinical recovery had been achieved and confirmed clinically. The presence of an exacerbation was defined in accordance with established consensus (26).

The fourth cohort was the *Pseudomonas aeruginosa* eradication cohort: to quantify the effect of targeted antimicrobial eradication therapy on the resistome, individuals with bronchiectasis were recruited at the bronchiectasis outpatient clinic of the fifth respiratory department of Sotiria Chest Hospital (Athens, Greece) with new *P. aeruginosa* infection defined by culture-based isolation from sputum for the first documented occasion. Patients were treated with 14 days of ciprofloxacin followed by sequential 3-month treatment with inhaled colistin in accordance with European Respiratory Society eradication recommendations (27). Spontaneous sputum sampling was performed at baseline, before antimicrobial treatment, and after eradication. Baseline and follow-up samples were assessed by *P. aeruginosa*-specific quantitative PCR (qPCR) and metagenomics (see online supplement).

A schematic figure summarizing all cohorts and the overall study design is provided in the online supplement (Figure E1 in the online supplement), together with details on ethics approvals and clinical, radiological, and functional evaluation of all participants.

Whole-Genome Shotgun Analysis of the Airway Resistome

Sputum DNA was extracted and its integrity confirmed before shotgun sequencing on a HiSeq 2500 platform. Adapter and quality trimming was performed using Trimmomatic, with nonhuman reads identified via Bowtie2 alignment against the

human genome (28, 29). For resistome profiling, nonhost reads were analyzed for ARGs using ShortBRED against the Comprehensive Antibiotic Resistance Database (CARD) to quantify ARG abundance (30, 31). We define “resistome” as the ARG profile observed in each patient, and “resistotype” denotes specific clusters or groupings within the resistome characterized by distinct resistance gene profiles, delineated by spectral clustering of Bray-Curtis distances, defined by maximal silhouette score. See online supplement for further details on sputum collection, DNA extraction, metagenomics sequencing, and additional downstream bioinformatic analysis. Negative controls for sequencing are illustrated in Figure E2, and raw data have been uploaded to the National Center for Biotechnology Information Sequence Read Archives under the project accession numbers PRJNA595703, PRJNA590225, and PRJNA982297.

Statistical Analysis

Distributional differences in patient demographic data were assessed using the Wilcoxon test (nonparametric) for continuous variables and the χ^2 test for categorical data (Table 1). A P value less than 0.05 was considered statistically significant for these tests. For group comparisons of differential resistance gene categories (normalized by relative abundance), the Kruskal-Wallis test was employed to assess nondiseased subjects and those with bronchiectasis as well as across clinical subgroups of the CAMEB 2 cohort, with statistical significance set at a false discovery rate-adjusted P value less than 0.05. Antimicrobial resistome, microbiome, and virome relative abundance profiles were visualized by stacked bar plots or principal coordinates analysis plots of Bray-Curtis dissimilarity. Permutational multivariate ANOVA (PERMANOVA) on derived patient-dissimilarity matrices was employed across relative groups in cross-sectional analysis. Geographic variability in the CAMEB 2 cohort was assessed by PERMANOVA, adjusting for major geographic covariates (identified in Table 1), with a significance threshold of $P < 0.05$ used to assess the overall effect of geography on the resistome. In longitudinal analyses, paired PERMANOVA was employed to account for within-patient variability across repeated measures to assess for temporal variation in response to antimicrobial

Table 1. Demographic Characteristics in the CAMEB 2 Bronchiectasis Cohort and Controls

Characteristic	Nondiseased (n = 25)	Bronchiectasis (n = 251)	Matched (n = 209)		P Value*
			SG-KL (n = 97)	DD-MI (n = 112)	
Geographic origin					
Singapore	25 (100%)	95 (38%)	62 (64%)	0	—
Kuala Lumpur	0	35 (14%)	35 (36%)	0	
Dundee	0	96 (38%)	0	88 (79%)	
Milan	0	25 (10%)	0	24 (21%)	
Matching criteria					
Median (IQR) age, yr	34 (30–39)	65 (59–73)	67 (59–74)	64 (59–72)	ns
Sex					
Male	14 (56%)	101 (40%)	38 (39%)	46 (41%)	ns
Female	11 (44%)	150 (60%)	59 (61%)	66 (59%)	
Exacerbator status					
0	—	85 (34%)	33 (34%)	34 (30%)	ns
1–2	—	108 (43%)	41 (42%)	49 (44%)	
≥3	—	58 (23%)	23 (24%)	29 (26%)	
Median (IQR) FEV ₁ % predicted	100 (96–109)	72 (56–87)	71 (56–84)	76 (61–94)	ns
Other disease characteristics (not matched)					
Disease severity					
Severe (BSI ≥9)	—	143 (57%)	62 (64%)	61 (54%)	ns
Moderate (BSI 5–8)	—	74 (29.5%)	24 (25%)	33 (30%)	
Mild (BSI 0–4)	—	34 (13.5%)	11 (11%)	18 (16%)	
Median (IQR) BMI, kg/m ²		22 (18–27)	19 (18–20)	27 (22–29)	<0.001 [†]
Etiology					
Idiopathic	—	157 (62.5%)	70 (72.2%)	75 (67%)	0.001 [†]
Postinfection	—	34 (13.5%)	10 (10.3%)	18 (16%)	
Posttuberculosis	—	13 (5%)	9 (9.3%)	0	
Other	—	47 (19%)	8 (8.2%)	19 (17%)	
MRC dyspnea score					
1–3	—	228 (91.6%)	91 (96%)	96 (86%)	0.042 [§]
4	—	19 (7.6%)	4 (4%)	14 (13%)	
5	—	2 (0.8%)	0	2 (1%)	
Radiological severity					
1 or 2 lobes involved	—	93 (38%)	28 (30%)	55 (49%)	0.022 [§]
> 3 lobes involved	—	154 (62%)	65 (70%)	57 (51%)	
Hospital admission in 1 yr before study recruitment					
Yes	—	98 (39%)	50 (52%)	30 (27%)	<0.001 [†]
No	—	153 (61%)	47 (48%)	82 (73%)	
Pseudomonas colonization					
Yes	—	35 (14%)	14 (14%)	16 (14%)	ns
No	—	216 (86%)	83 (86%)	96 (86%)	
Colonization with other organisms					
Yes	—	89 (36%)	37 (38%)	15 (13%)	<0.001 [†]
No	—	162 (64%)	60 (62%)	97 (87%)	
Bronchodilator use					
Yes	—	119 (47%)	47 (48%)	57 (51%)	ns
No	—	132 (53%)	50 (52%)	55 (49%)	
Inhaled corticosteroids					
Yes	—	99 (39%)	18 (19%)	66 (59%)	<0.001 [†]
No	—	152 (61%)	79 (81%)	46 (41%)	
Long-term antibiotics					
Yes	—	61 (24%)	14 (14%)	30 (27%)	0.044 [§]
No	—	190 (76%)	83 (86%)	82 (73%)	

Definition of abbreviations: BMI = body mass index; BSI = Bronchiectasis Severity Index; CAMEB 2 = Cohort of Asian and Matched European Bronchiectasis 2; DD-ML = Dundee + Milan cohort; MRC = Medical Research Council; ns = nonsignificant; SG-KL = Singapore + Kuala Lumpur cohort.

*P values indicated for relevant comparisons (Singapore + Kuala Lumpur vs. Dundee + Milan).

[†]P < 0.001, [‡]P < 0.01, and [§]P < 0.05.

treatment, also using a threshold of $P < 0.05$. Spectral clustering was performed on Bray-Curtis distance between patient ARG profiles, with the stability and robustness of the clusters evaluated by maximizing average silhouette scores (32). Differential abundance of resistance genes was assessed using linear discriminant analysis effect size with default parameters, with a threshold for significance set at a linear discriminant analysis score (\log_{10}) of 2.0 or higher (33). Cramer's V and the contingency coefficient were calculated as measures of the strength of association between nominal clinical variables, with a significance level of $P < 0.05$. All statistical analysis was performed using custom scripts written in R. A repository describing all processed datasets and analytical codes to reproduce results described in this manuscript (including R package version numbers) is accessible at GitHub (<https://github.com/RespiratoryMicrobiome/BE-Resistome>).

Results

In our initial comparison of patients from CAMEB 2 ($n = 251$) with our nondiseased comparator group (unmatched, $n = 25$), the bronchiectasis resistome was characterized by distinct ARG profiles. These encompassed a range of drug classes, notably including therapeutic antibiotic agents such as aminoglycosides, β -lactams, fluoroquinolones, and tetracyclines, alongside natural products not primarily developed for therapeutic use, such as acridine dyes, antibacterial free fatty acids, bicyclomycin, and triclosan. Resistome signatures in bronchiectasis exhibited marked increases in the relative abundance of multidrug and aminoglycoside resistance genes as well as genes encoding for resistance to phenicol, triclosan, and peptide antibiotic agents of lesser direct therapeutic relevance (PERMANOVA, $P < 0.001$; Figures 1A and 1B). When assessed longitudinally in repeated-measures analyses during stable disease (Figure 1C) or across exacerbations (Figures 1D and 1E), temporal within-patient resistome profiles demonstrated temporal stability in the bronchiectasis exacerbation cohort ($n = 21$). In contrast, between-patient profiles differed significantly and exhibited significant association with time to the next exacerbation (PERMANOVA, $P = 0.026$; Figures 1F and 1G). Here, individuals experiencing shorter intervals between

exacerbations exhibited a distinct resistome profile (paired PERMANOVA, $P < 0.05$) and an apparent increasing trend related to the ratio of multidrug to macrolide resistance genes (Figures 1F and 1G). Taken together, within-patient resistome dynamics appear temporally stable, whereas between-patient variation exists and is associated with shorter intervals between exacerbations in bronchiectasis in the longitudinal exacerbation cohort.

Having established resistome stability over time and during exacerbations, we next sought to explore the relationship between resistome profiles and key clinical features of bronchiectasis extant in the CAMEB 2 cohort (Figure 2). By assessing the abundance of resistance genes (grouped by drug class), we identified significant associations between several resistance gene classes and exacerbation frequency, lung function, and underlying bronchiectasis etiology in the cross-sectional CAMEB 2 cohort (Kruskal-Wallis $P < 0.05$, false discovery rate-corrected). However, importantly, no association with bronchiectasis severity per the Bronchiectasis Severity Index was observed (Figure 2). Variability in resistome profiles was most evident at phenotypic extremities, with frequent exacerbators (i.e., those experiencing at least three exacerbations in the preceding 1 yr) exhibiting significant differences in aminoglycoside, bicyclomycin, phenicol, and triclosan resistance (Figure 2A). Individuals with the poorest lung function (i.e., $FEV_1 < 50\%$ predicted) exhibited increased bicyclomycin, triclosan, peptide, sulfonamide, and multidrug resistance (Figure 2B), while, interestingly, underlying aetiology also associated with an altered resistome, largely conferred by β -lactam and fosfomycin resistance in those with post-tuberculosis bronchiectasis (Figure 2D).

Having determined that resistomes show associations with exacerbation frequency, poorer lung function, and underlying etiology in bronchiectasis, we next sought to interrogate the relationship with etiology because this is an established contributor to clinical and geographic heterogeneity observed in large bronchiectasis registry studies (34, 35). To achieve this, we leveraged the matched design of the prospectively recruited CAMEB 2 cohort, which includes patients from Asia (Singapore and Kuala Lumpur, Malaysia) who were matched on age, sex, exacerbation

frequency, and lung function with patients recruited from two European sites (Dundee, Scotland; and Milan, Italy) ($n = 209$; Figure 3A and Table 1). Importantly, the CAMEB 2 cohort differs from the original CAMEB cohort that matched patients on age, sex, and disease severity and found the latter factor not to be related to differences in resistome profiles (Figure 2C) (23, 32, 36, 37). Therefore, by design, CAMEB 2 allowed matching of patients based on exacerbation frequency and lung function, which are both independently related to resistome profiles (c.f. Figures 2A and 2B) across geographic regions, allowing for a deeper exploration of the true associations between etiology and resistomes (Figure 3A). Within the CAMEB 2 cohort, significant geographic covariates were observed, including median body mass index, etiology, radiological severity, hospital admissions, and colonization with organisms other than *Pseudomonas* species. Additionally, inhaled corticosteroid use and long-term antibiotic use showed significant differences, being more common in the European group (Table 1). Bronchiectasis etiology and geographic patient origin were tightly linked (38, 39), and, notably, etiology was strongly correlated with geographic patient origin, representing an important covariate ($\chi^2 = 42.6$, degrees of freedom = 9; $P < 0.001$) with moderate association indicated by Cramer's V ($V = 0.29$) and contingency coefficients ($C = 0.449$) in matched subjects of CAMEB 2. Assessment of bronchiectasis resistomes at the level of individual genes demonstrated a highly significant effect for geographic patient origin ($P = 0.006$), one that remained even after accounting for etiology (Figure 3B). PERMANOVA also confirmed body mass index ($P = 0.040$) and etiology ($P = 0.020$) as significant predictors. These results indicate that geographic differences, alongside individual health characteristics, play a significant role in the variability of ARGs. Despite geographic variability in therapy, the resistome was not significantly different in users of inhaled corticosteroids and/or long-term macrolides (Figure E3).

Interestingly, although Singapore and Kuala Lumpur appear to have overlapping resistome profiles, Dundee and Milan, both in Europe, appeared different, in line with the reported variation in bronchiectasis across Europe in the European Multicentre Bronchiectasis Audit and Research Collaboration (EMBARC) registry

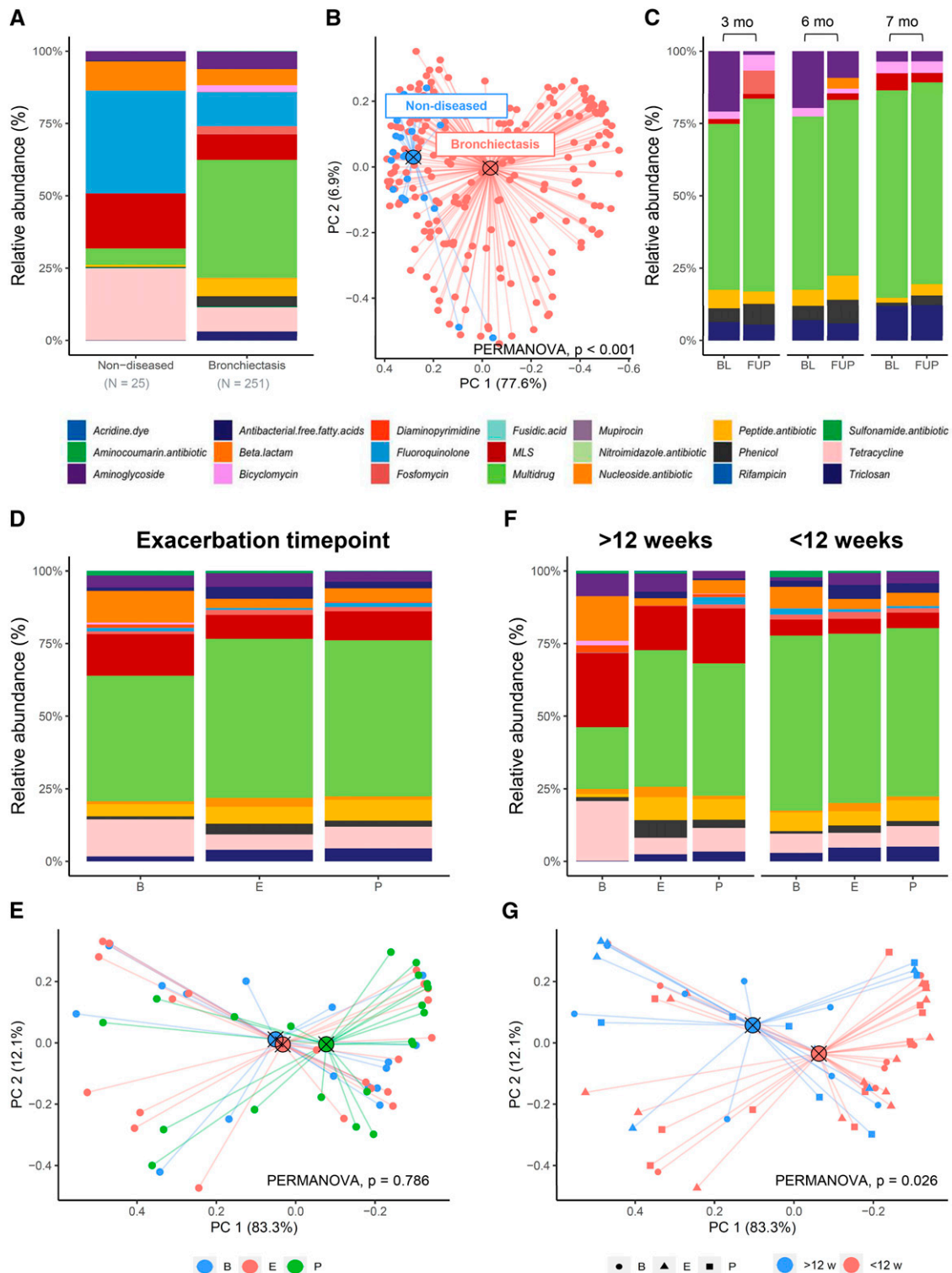


Figure 1. Characterization of the bronchiectasis resistome. (A) Stacked bar plots representing the observed resistome profiles in bronchiectasis ($n = 251$; Cohort of Asian and Matched European Bronchiectasis 2) compared with a nondiseased comparator cohort ($n = 25$). Stacked bars represent the relative abundance of resistance genes grouped according to drug class. (B) β -Diversity of resistance gene profiles (i.e., Bray-Curtis distance) assessed by principal coordinate analysis (PCoA) illustrating resistome diversity and colored by cohort: nondiseased in blue and bronchiectasis in red (permutational multivariate ANOVA, $P < 0.001$). (C) Longitudinal resistome dynamics in stable bronchiectasis assessed at baseline and follow-up time points across varying time intervals (left; 3 mo, center; 6 mo, right; 7 mo). (D and E) Prospective longitudinal analysis of resistome profiles during exacerbations of bronchiectasis ($n = 18$, cohort 3, "exacerbation" cohort) with sampling at

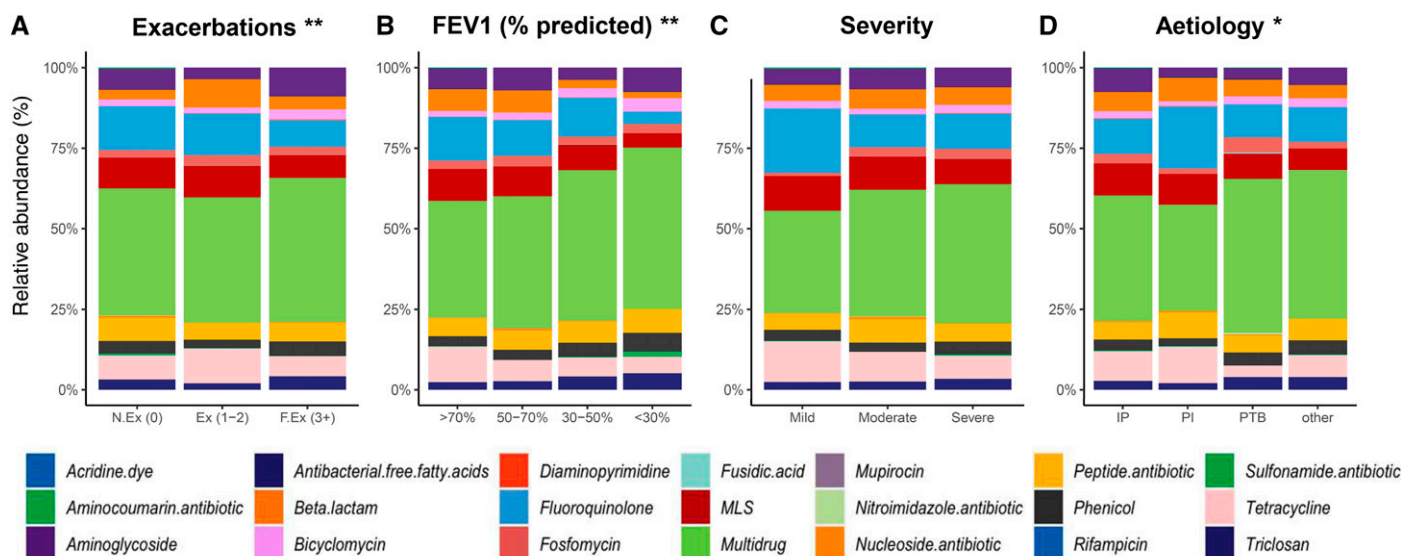


Figure 2. Association between resistome composition and clinical features in bronchiectasis. Stacked bar plots representing resistome profiles in stable bronchiectasis in the Cohort of Asian and Matched European Bronchiectasis 2 (matched and unmatched, $n = 251$) stratified according to: (A) exacerbation status, i.e., number of exacerbations in the preceding year categorized as nonexacerbators (i.e., no exacerbations), exacerbators (one or two exacerbations), or frequent exacerbators (at least three exacerbations); (B) lung function based on FEV₁% predicted as >70%, 50–70%, 30–50%, and <30% predicted; (C) disease severity based on the Bronchiectasis Severity Index (BSI) as mild (BSI = 0–4), moderate (BSI = 5–9), or severe (BSI ≥ 9); and (D) bronchiectasis etiology as idiopathic, postinfection, posttuberculosis, or other. Assessment of intergroup differences in relative abundance of antimicrobial resistance gene classes was evaluated using the Kruskal-Wallis test with false discovery rate correction: * $P < 0.05$ and ** $P < 0.01$. Ex = exacerbators; F.Ex = frequent exacerbators; IP = idiopathic; PI = postinfection; PTB = posttuberculosis.

(Figure 3B) (35). In contrast, etiological association with resistance gene profiles failed to reach statistical significance in PERMANOVA analysis of matched patients, suggesting that resistomes relate most strongly to a patient's country of origin rather than underlying etiology (Figure 3C). Reported ancestries are related to country of origin and varied within Singapore (76% Chinese) and Kuala Lumpur (68% Malay) relative to Scotland and Italy, both of which had 100% European ancestry. We failed to detect any significant differences in resistome composition associated with within-region ethnic diversity ($P = 0.636$). Resolution to individual ARGs reveals that individuals recruited to CAMEB 2 from Europe could be distinguished by the presence of specific multidrug and fluoroquinolone resistance genes *hmrM* and *pataA* and the tetracycline

resistance gene *tetO* (Figure E4). Conversely, Asian participants in CAMEB 2 exhibited an increased prevalence of broad-spectrum multidrug efflux systems as well as the macrolide resistance gene *ErmF*, aminoglycoside resistance genes [*APH(3'')-Ib* and *APH(3')-Ib*], and β -lactam (*CfxA2*) and fluoroquinolone (*oqxAB*) resistance mechanisms (see Figure E4), reflecting a diversity of resistance potential related to geographic origin. Lung microbiomes are intricately linked to resistomes, as resident microbes express ARGs that contribute to the resistome (10). Consequently, lung microbiomes from CAMEB 2 exhibit significant geographic variability based on country of origin (Figures E5A and E5B), in line with comparable findings from resistome analysis (Figure 3B), whereas no such relationship was evident in a

comparison of etiologies (see Figures E5C and E5D). Most noticeably, individuals from Asia exhibited a higher relative abundance of *Klebsiella pneumoniae* whereas Europeans exhibited marked increases in *Haemophilus influenzae* (see Figures E5A and E5B). Finally, we applied a metagenomic pipeline for the analysis of viral content (i.e., DNA viruses) (see online supplement and Figure E6) to evaluate for bacteriophages that may be contributing to our findings. Bacteriophages belonging to the families Iridoviridae, Siphoviridae, Myoviridae, Phycodnaviridae, and Polydnviridae are detectable in bronchiectasis and include several streptococcal, pseudomonal, and staphylococcal phages; however, when considered independently, bacteriophage profiles did not demonstrate any significant or direct relationships with clinical outcomes

Figure 1. (Continued). baseline (before exacerbation, during exacerbation, and 2 wk after exacerbation following antibiotic treatment). (F and G) Prospective longitudinal analysis of resistome profiles in the bronchiectasis exacerbation cohort grouped by observed time to the next exacerbation as <12 weeks or >12 weeks, respectively. PCoA of resistome (β -diversity (i.e., Bray-Curtis distance) comparing (E) time points across an exacerbation and (G) time to the next exacerbation are illustrated below their respective stacked bar plots (D and F). P values for permutational multivariate ANOVA comparing groups are illustrated. Central points intersected by a cross indicate the centroid in PCoA visualizations. B = before exacerbation; BL = baseline; E = during exacerbation; FUP = follow-up; P = 2 weeks after exacerbation following antibiotic treatment; PC = principal coordinate; PERMANOVA = permutational multivariate ANOVA.

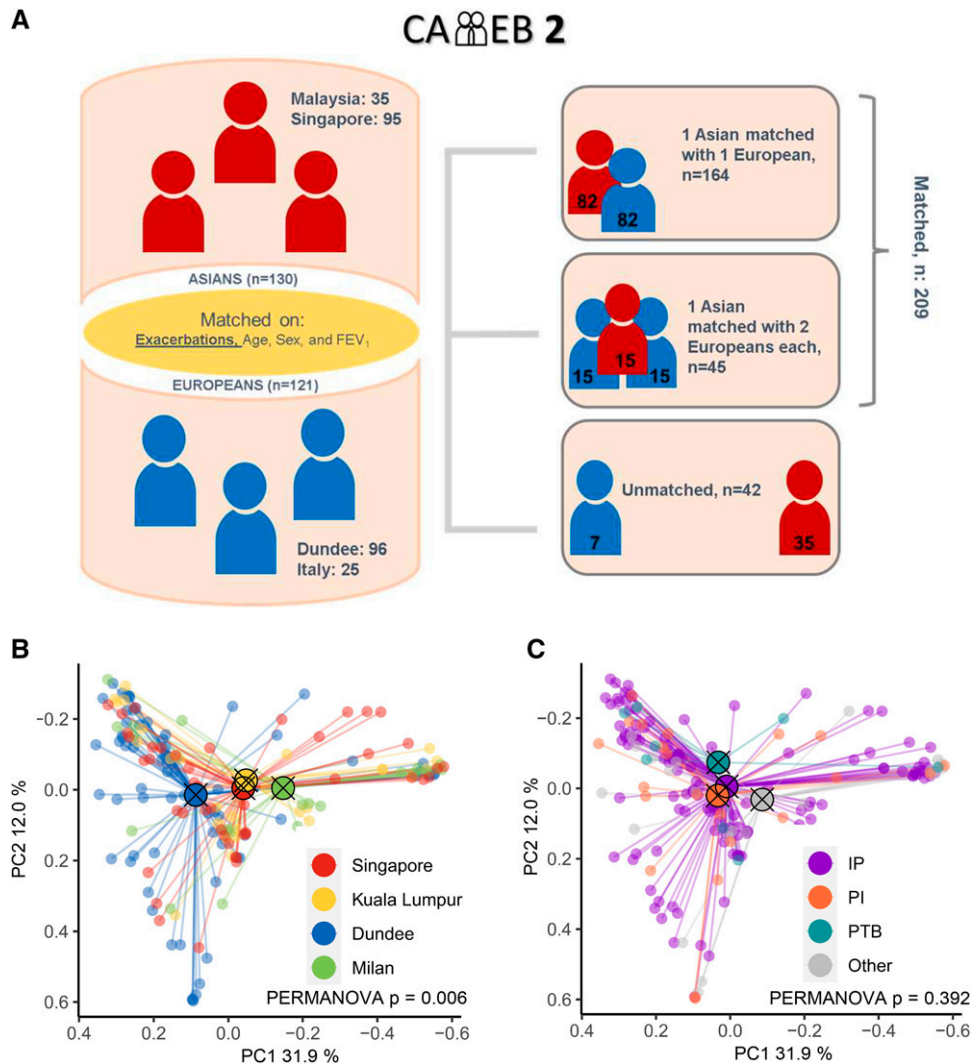


Figure 3. The Cohort of Asian and Matched European Bronchiectasis 2 (CAMEB 2) cohort and geographic variability in the bronchiectasis resistome. (A) Schematic overview of the matching strategy employed for individuals included in CAMEB 2. Asian patients (Singapore, $n=95$; and Kuala Lumpur, Malaysia, $n=35$) were compared with European patients (Dundee, Scotland, $n=96$; and Milan, Italy, $n=25$) to identify a cohort of 209 patients matched for age, sex, exacerbation frequency, and lung function differing in geographic origin. (B) β -Diversity of resistance gene profiles (i.e., Bray-Curtis distance) assessed by principal coordinate analysis (PCoA) illustrating resistome diversity and colored by geographic origin assessing matched patients from CAMEB 2: Singapore (red), Kuala Lumpur (yellow), Dundee (blue), and Milan (green) (permutational multivariate ANOVA, $P=0.006$). (C) β -Diversity of resistance gene profiles (i.e., Bray-Curtis distance) assessed by PCoA illustrating resistome diversity and colored by etiology assessing matched patients from CAMEB 2: idiopathic (purple), postinfection (orange), posttuberculosis (blue), and others (gray). Central points intersected by a cross indicate the centroid in PCoA visualizations. IP = idiopathic; PC = principal coordinate; PERMANOVA = permutational multivariate ANOVA; PI = postinfection; PTB = posttuberculosis.

of interest. They did vary based on geographic patient origin, in line with our prior findings (Figure E7).

Because the bronchiectasis resistome likely contains signatures amenable to improving patient risk stratification, we next performed an unsupervised analysis of resistome profiles observed in the CAMEB 2 cohort, leading to the identification of two distinct “resistotype” clusters, RT1 and RT2 (Figures 4A and 4B), delineated by spectral

clustering of Bray-Curtis distances, with a mean misclassification ratio of 3.4%, indicating a cluster robustness of 96.6% (based on 100 bootstrap iterations). Comparable microbial read depths were observed across both clusters, suggesting minimal influence of sequencing depth, despite a significant association with ARG diversity across patient samples (Figure E8). The RT1 cluster was broadly defined by an increased abundance of genes conferring

resistance to tetracyclines, β -lactams, and macrolide-lincosamide-streptogramin B class (MLS) antibiotics. RT2 exhibits an increased relative abundance of aminoglycoside, phenicol, and multidrug resistance genes as well as genes conferring resistance to peptide, fosfomycin, and bicyclomycin antibiotics (Figure 4A). Correlative gene-specific linear discriminant analysis (effect size) highlights fluoroquinolone-, tetracycline-, and MLS-specific resistance genes as characteristic

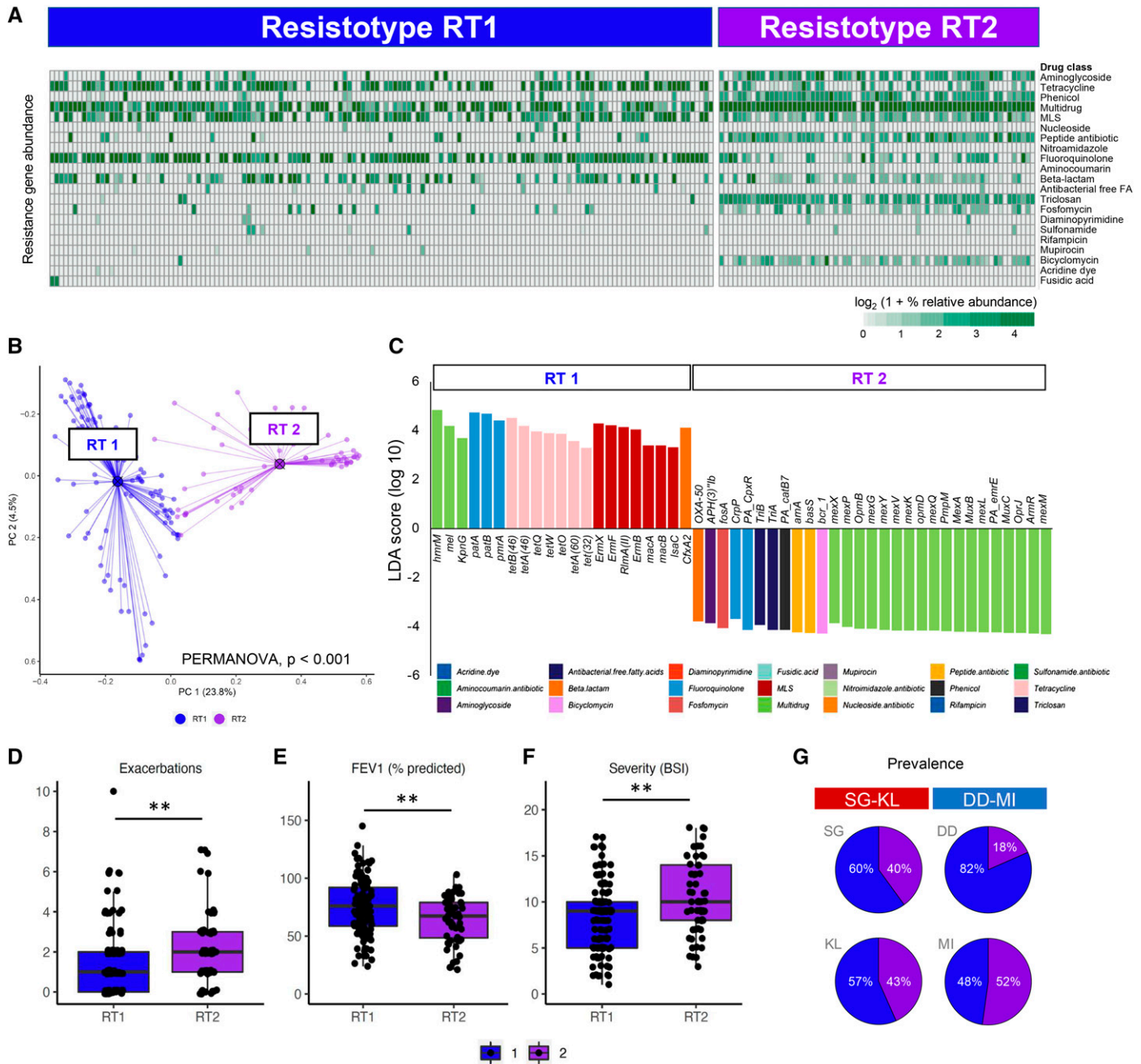


Figure 4. Characterization of bronchiectasis resistotypes. (A) Heat map illustrating the Cohort of Asian and Matched European Bronchiectasis 2 resistome profiles that associate with the identified resistance gene profile clusters (“resistotypes” [RTs]) indicated as RT1 (blue) and RT2 (purple). The heat map details the resistance gene composition of each resistotype cluster at the drug class level, expressed as \log_2 percentage relative abundance. (B) Principal coordinate analysis of gene-level resistome profiles demonstrating the distinct resistotype RT1 and RT2 clusters as defined by β -diversity of resistance gene profiles (i.e., Bray-Curtis distance). Circles intersected by a cross indicate principal coordinate analysis centroids of compared groups (permutational multivariate ANOVA, $P < 0.001$). (C) Linear discriminant analysis highlighting resistance genes that distinguish the RT1 and RT2 resistotype clusters. (D–F) Analysis of clinical features associated with the resistotype clusters RT1 (blue) and RT2 (purple) including (D) exacerbation frequency in the year preceding recruitment, (E) lung function (as FEV₁% predicted), and (F) disease severity (per Bronchiectasis Severity Index). (G) Prevalence of the resistotypes across the recruited cohorts and respective geographic regions. ** $P < 0.01$. BSI = Bronchiectasis Severity Index; DD = Dundee, Scotland; KL = Kuala Lumpur, Malaysia; LDA = linear discriminant analysis; MI = Milan, Italy; PERMANOVA = permutational multivariate ANOVA; SG = Singapore.

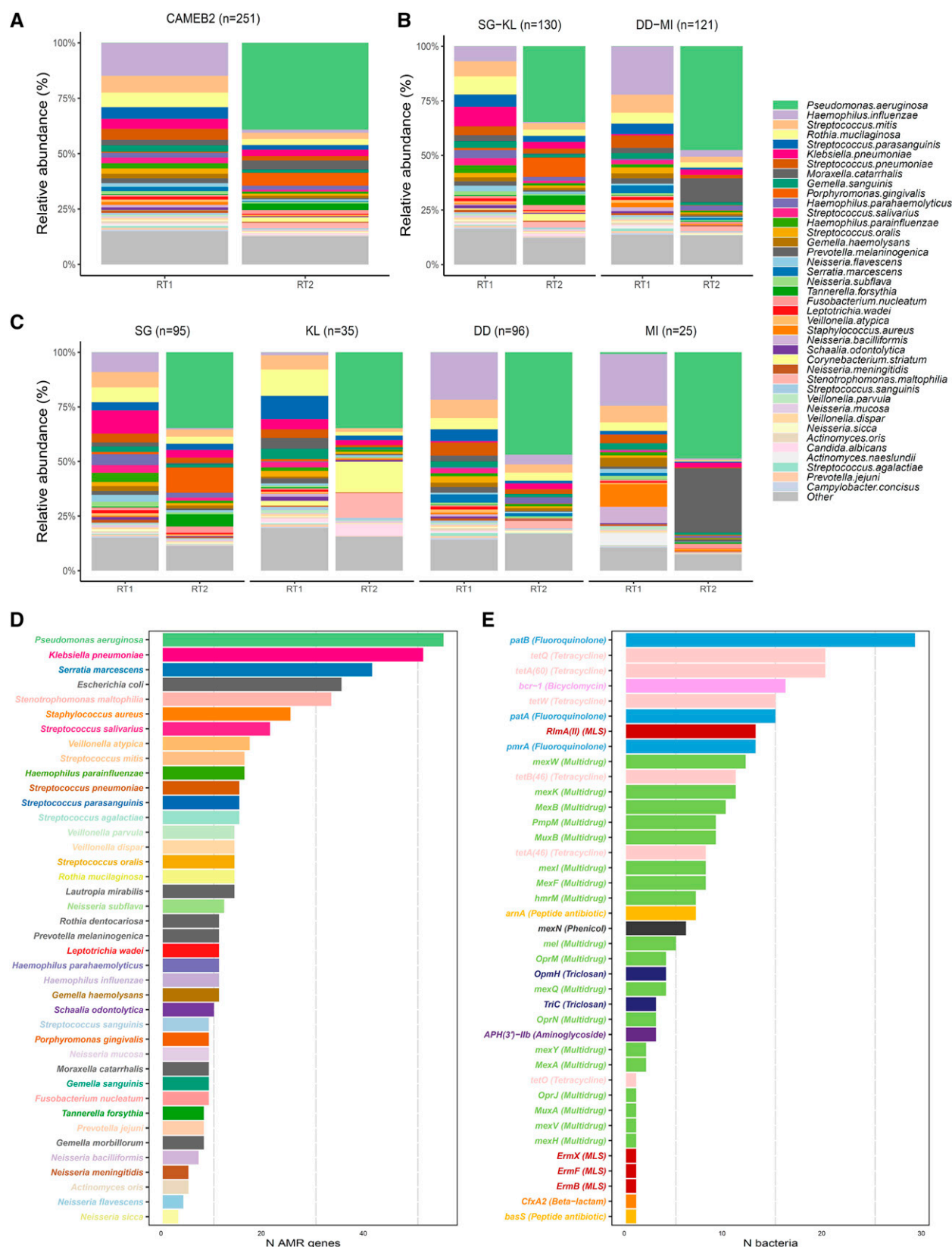


Figure 5. Microbiome correlates of bronchiectasis resistotypes (RTs) RT1 and RT2. Stacked bar plots illustrating the relative abundance of microbial taxa associated with (A) resistotypes RT1 and RT2 and stratified by (B) continent and (C) country of origin. (D) Analysis of resistance

of RT1, whereas RT2 is defined by aminoglycoside, phenicol, bicyclomycin, and, most strikingly, multidrug resistance genes (Figure 4C). Importantly, the identified resistotypes significantly associate with clinical outcomes in bronchiectasis, with RT2 associated with increased exacerbations, poorer lung function, and greater disease severity (Figures 4D–4F). Interestingly, resistotypes were not evenly distributed across recruitment sites, with Dundee exhibiting the lowest proportion of patients with RT2 compared with Singapore, Kuala Lumpur, and Milan, respectively, corroborating our previously described geographic differences (Figure 4G). Genes encoding resistance to antimicrobial agents such as triclosan, phenicol, and certain peptide classes, which are not widely used in clinical settings, suggest that environmental factors and potentially indirect selection pressures may play a role in shaping resistomes.

We next evaluated microbiomes associated with the observed resistotypes and found that RT1 is characterized by increased abundance of *H. influenzae*, *Rothia mucilaginosa*, and several *Streptococcus* species, whereas RT2 is distinguished by a predominance of *P. aeruginosa* and *K. pneumoniae* (Figures 5A–5C). The observed relationship between *P. aeruginosa* and *H. influenzae* is further supported by quantitative data confirming increased ratios of *P. aeruginosa* to *H. influenzae* microbial burden within RT2, determined by confirmatory qPCR analysis, further underscoring resistome–bacteriome associations (Figure E9). Apparent exceptions were noted, such as *H. influenzae* dominance in some RT2 patients and *P. aeruginosa* dominance in some RT1 patients by qPCR, illustrating a further level of complexity to interpreting microbe–resistome dynamics (see Figure E9). In addition, 10 patients in the RT1 cluster exhibited *P. aeruginosa* positivity by microbial culture. To disentangle the potential effects of *P. aeruginosa* and resistomes on the observed disease

outcomes associated with RT2, we performed subanalyses excluding all *P. aeruginosa*–positive patients (14%). Results were consistent with our initial analysis (Figure 4), except for exacerbations that trended toward significance (Figure E10).

In addition to short-read taxonomic classification (through ShortBRED and Kaiju classifiers [31, 40]), we additionally performed metagenomic contig assembly to define the genetic context of the identified resistance genes and further elucidate taxonomic associations. This allowed us to describe the number of resistance genes associated with each major bacterial taxon in bronchiectasis as well as the distribution of the most prevalent genes across these bacteria (Figures 5D and 5E). Several major bacterial taxa exhibit a high abundance of resistance genes, including *P. aeruginosa*, *K. pneumoniae*, *Serratia marcescens*, and *H. influenzae*. Highly notable were the more than 50 mapped resistance genes in *P. aeruginosa* and *K. pneumoniae*; other less abundant species included *Escherichia coli*, *Stenotrophomonas maltophilia*, and *Staphylococcus aureus*, which all exhibit extensive resistance gene repertoires (Figure 5D). Commensals including *Streptococcus*, *Neisseria*, *Veillonella*, *Rothia*, and *Prevotella* were all shown to be important carriers of AMR in bronchiectasis (Figure 5D). Among the most widely distributed resistance genes were the fluoroquinolone resistance genes *patA* and *patB*, observed in association with as many as 15 and 29 distinct bacterial species, respectively, and both associated with RT1. Other resistance genes associated with RT1 [i.e., *patA*, *patB*, *tetQ*, *tet60(A)*, *tetW*, *rlmA(II)*, *tet46(B)*, and *pmrA*; cf. Figure 4C] were among the most widely distributed across bacterial taxa (present in ≥ 10 species), whereas those associated with RT2 were overall less widely distributed, with the exception of *bcr-1*, *pmpM*, and *mexB*, respectively (Figure 5E). Altered microbial interaction metrics were observed in the RT2 cluster that exhibited overall increased

interactions (142 vs. 70). Notably, the observed interaction network implicates *P. aeruginosa* and *K. pneumoniae* (among others, including *R. mucilaginosa*) as keystone microbes of this resistotype. Corresponding decreases in several commensal taxa, including streptococci, fusobacteria, and Veillonellaceae, were observed, all of which represent important nodes for the RT1 interaction network (Figure E11).

Having determined the clinical relevance of bronchiectasis resistotypes, we next assessed if targeted therapeutic intervention with antibiotic agents can influence the resistome and its underlying resistotype. To investigate this, we prospectively studied eight culture-positive *P. aeruginosa*–infected individuals undergoing protocol-driven *P. aeruginosa* eradication involving an initial 2-week treatment with oral ciprofloxacin followed by nebulized colistin for three consecutive months (longitudinal bronchiectasis eradication cohort). Sampling for analysis was obtained at baseline (before eradication) and then at 6 months after eradication therapy ($n = 8$ patients with 16 samples). Successful eradication of *P. aeruginosa* was confirmed by qPCR verifying eradication in five of the eight patients and a reduction in *P. aeruginosa* burden in all but a single patient (Figure E12). This was accompanied by a reduction in the relative abundance of *P. aeruginosa* by metagenomic analysis from 32% (IQR, 15–67%) before eradication to 1.7% (IQR, 0–5%) after eradication (Figure 6A). Concomitant increases in the relative abundance of *Haemophilus* spp., several *Streptococcus* spp., and *K. pneumoniae* (in a single patient) were apparent after eradication (Figure 6A). These microbial changes were accompanied by appreciable shifts in resistome profiles whereby the ratio of multidrug to MLS resistance gene abundance decreased upon completion of eradication therapy (Figure 6B). Interestingly, resistome profiles observed in the pre- versus posteradication therapy states bore remarkable resemblance

Figure 5. (Continued). gene content among the top microbial taxa identified in the Cohort of Asian and Matched European Bronchiectasis 2. Horizontal bars indicate the number of antimicrobial resistance genes (x-axis) identified on contigs assigned to the indicated bacterial taxa (y-axis) based on metagenomic assembly. Prevalent bacterial taxa ranked within the top 40 (by average relative abundance) are colored, whereas lower-abundance taxa are grayed. (E) Analysis of resistance gene distribution across bacterial taxa. Horizontal bars indicate the number of bacterial taxa (x-axis) expressing the respective indicated resistance genes (y-axis) based on metagenomic contig analysis. Resistance genes are differentiated by color according to drug class as indicated in the labels on the y-axis (in parentheses). AMR = antimicrobial resistance; DD = Dundee, Scotland; KL = Kuala Lumpur, Malaysia; MI = Milan, Italy; SG = Singapore.

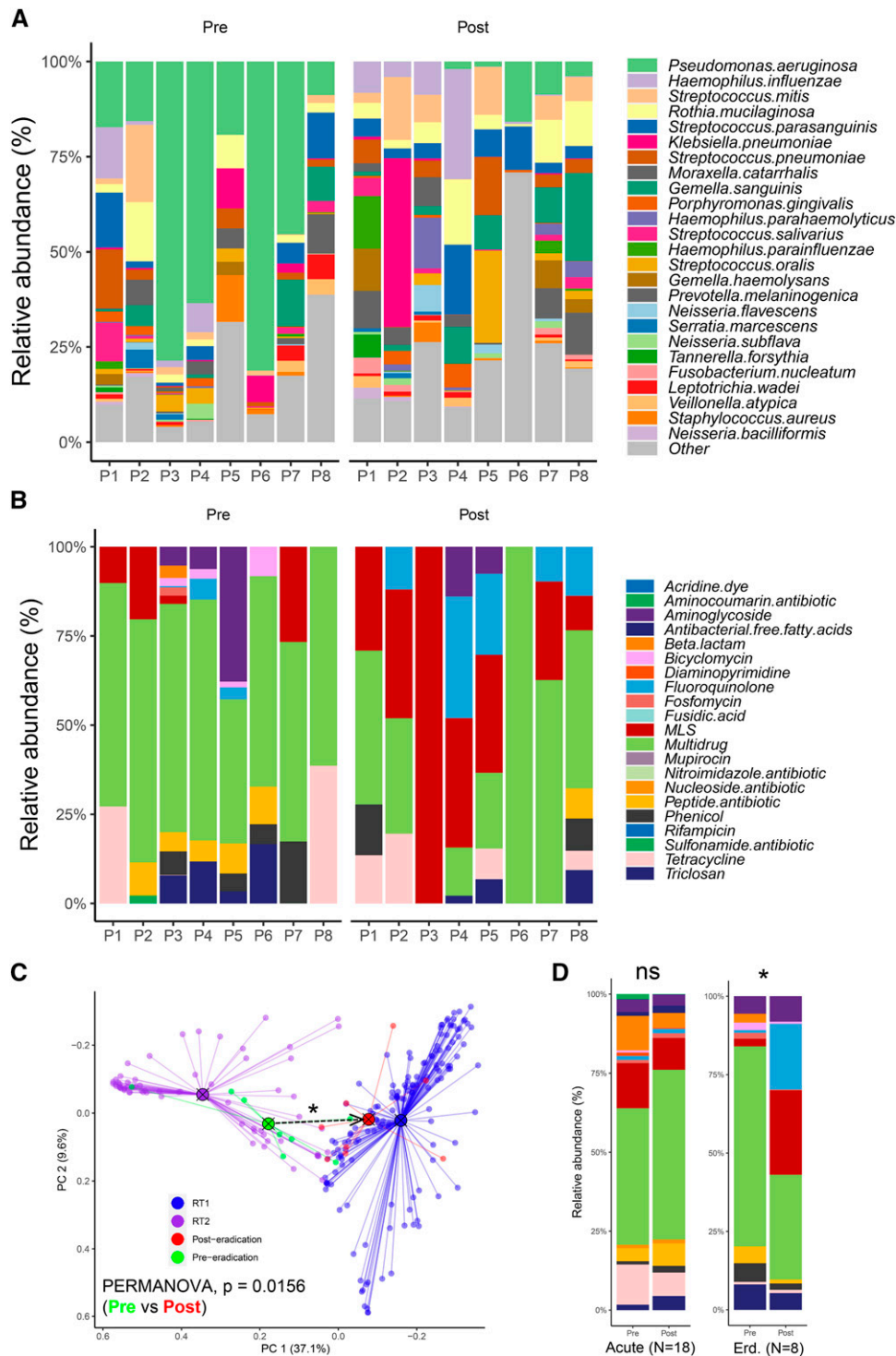


Figure 6. The effect of *Pseudomonas aeruginosa* eradication therapy on bronchiectasis resistotypes. (A) Microbiome composition of eight patients with *P. aeruginosa* culture-positive bronchiectasis (P1–P8) receiving eradication therapy with 14 days of oral ciprofloxacin followed by 3 months of nebulized colistin. Stacked bar plots illustrate the lung microbiome composition before and after eradication therapy. (B) Resistome profiles of patients with *P. aeruginosa* culture-positive bronchiectasis (P1–P8) receiving eradication therapy with 14 days of oral ciprofloxacin followed by 3 months of nebulized colistin. Stacked bar plots illustrate resistome composition (at drug class level) before and after eradication therapy. (C) Principal coordinate analysis plot illustrating resistome gene profiles incorporating patients undergoing *P. aeruginosa* eradication therapy (before eradication, green; after eradication, red) oriented to their previously determined resistotype clusters: RT1 (blue) and RT2 (purple). A black arrow indicates the trajectory of the eradication therapy group centroids, illustrating a shifting proximity from the initial RT2 (purple)

to the RT2 and RT1 clusters, respectively, as previously characterized (*c.f.* Figure 4A), with overrepresentation of multidrug resistance genes in the preeradication state (RT2-like) compared with a greater abundance of MLS and fluoroquinolone resistance genes in the posteradication state (RT1-like). The average number of identified resistance genes was lower after eradication therapy (9 vs. 13), as was resistance gene diversity (average Shannon diversity index, 1.6 vs. 2.3). In contrast to acute antibiotic bursts to treat acute exacerbations (*c.f.* Figure 1D), these findings suggest that prolonged and targeted eradication therapy causes appreciable shifts in resistome profiles and can potentially mediate reversion from an unfavorable RT2 resistotype to an RT1 resistotype (Figure 6C). This is substantiated by the significant shift in β -diversity observed following eradication therapy in contrast to patients treated for acute exacerbation (*c.f.* Figures 1D and 1E), in whom no significant difference was observed (Figure 6D).

Discussion

The bronchiectasis microbiome exhibits resistance gene signatures linked to underlying taxonomic composition, with important clinical and therapeutic implications (2). Discordance between *in vitro* antimicrobial sensitivity testing of individual pathogens and clinical efficacy and outcome in practice is well recognized in bronchiectasis, evidenced by the repeated failure of antimicrobial clinical trials (5–9). Although many factors have been advanced to explain such inconsistency, the resistome, a collection of all ARGs within the host microbiome, offers new insight (4, 10, 32). Here, we performed the largest and most comprehensive analysis of the bronchiectasis resistome to date, including patients from five countries in clinically “matched” cohorts of Asian and European origin to evaluate its clinical significance.

The bronchiectasis resistome is distinct from that within a healthy lung, a likely consequence of microbial dysbiosis related

to recurrent cycles of exacerbation and antibiotic therapy (2). Interestingly, within-patient profiles remain stable over time and during exacerbations, suggesting that microbial dysbiosis, when established, remains, and can therefore be leveraged for prognosis, patient stratification, and precision therapy (32, 41–43). Importantly, between-patient resistome profiles markedly differ, allowing resistome signatures (at baseline) to associate with time to the next exacerbation. Individuals who exhibit a shorter time to the next exacerbation are associated with variable relative abundance of macrolide and multidrug resistance gene determinants, whereas an increased ratio of MLS to multidrug resistance was linked to more clinically favorable outcomes, bearing a similarity to the resistomes of nondiseased (healthy) controls. These findings are consistent with the prior identification of a core macrolide resistome even in healthy individuals (10, 44).

Exacerbation frequency is associated with poor clinical outcomes and mortality in bronchiectasis and remains a key endpoint in clinical trials (45, 46). Links between the bronchiectasis microbiome and exacerbation frequency are established and supported by prior clinical studies (32, 42, 47–49). Here, we reveal that the resistome profiles of patients with frequent exacerbations have distinct profiles characterized by increased abundance of ARGs related to aminoglycoside, bicyclomycin, phenicol, and triclosan resistance, a likely consequence of repeated and varied antimicrobial exposure over time. Whether such profiles can be leveraged for therapeutic decision-making in practice, especially in those with frequent exacerbations, is an important clinical and research question that necessitates future prospective study. Notably, resistome profiles further associate with other demographic and clinical parameters in bronchiectasis, including lung function and disease etiology; however, for the latter, this relationship is driven by geographic patient origin rather than etiology, a finding uncovered by leveraging the CAMEB 2 cohort that “matched” individuals across Asian and

European sites by age, sex, exacerbation frequency, and lung function. Using CAMEB 2 allowed detailed interrogation of the specific contributions of disease etiology and geographic patient origin to resistome dynamics by controlling for, through meticulous patient matching, exacerbation frequency and lung function, two other determinants of resistome composition. Our design thus addresses the comparison of diverse cohorts, overcoming challenges noted in previous studies (5, 7, 8).

Geographic variation remains a key determinant of the observed disease heterogeneity in bronchiectasis, which includes etiology, but also other features such as microbiology and the microbiome (2, 11, 13, 38, 50–52). The recent EMBARC report reveals that, even across a single continent, Europe, significant disease heterogeneity exists in microbiology, exacerbations, and treatment response (35). Reports from other regions, including the United States, Australia, India, and Korea, further affirm such inherent differences, which significantly contribute to the clinical variability and negative outcomes seen across clinical trials in bronchiectasis (5–9, 11, 34, 51, 53–55). Our microbiome results are consistent with the reports from EMBARC based on culture, specifically with the higher frequency of *H. influenzae* in Northern Europe, increased *P. aeruginosa* in Southern Europe, and higher *K. pneumoniae* in Asia all replicated here using next-generation sequencing (56). The interplay between these factors is complex and varies globally, suggesting that a deeper understanding of these relationships is crucial in clinical practice and future trial design, particularly in disentangling the independent effects of the resistome.

We next sought to establish unbiased signals within the bronchiectasis resistome conferring clinical and biological relevance for translational application. Unsupervised analysis of AMR profiles revealed two bronchiectasis resistotypes, RT1 and RT2, each demonstrating a distinct resistance pattern and clinical correlates. RT1 is

Figure 6. (*Continued*). to RT1 (blue) cluster in the pre- and posteradication state, respectively. (D) Stacked bar plots depicting antimicrobial resistome profiles of patients before and after antimicrobial treatment. The left section illustrates changes in these profiles following the administration of acute antibiotic therapy to treat pulmonary exacerbations; the right illustrates changes observed after *P. aeruginosa* eradication therapy. * $P < 0.05$. ns = not significant ($P > 0.05$ on paired permutational multivariate ANOVA); PERMANOVA = permutational multivariate ANOVA.

characterized by favorable clinical outcomes and fluoroquinolone, tetracycline, and MLS resistance, with microbiomes dominated by *H. influenzae*, *R. mucilaginosa*, and several *Streptococcus* species. RT1 exhibits resistome profiles characteristic of those observed in our nondiseased comparator cohort despite significant demographic differences, including age. Indeed, existing literature suggests a relative stability of the airway microbiome across age, suggesting that this may not be the primary factor driving pronounced bronchiectasis resistome signatures such as those seen in RT2 (57, 58). The RT2 resistotype is associated with more exacerbations, poorer lung function, and greater disease severity. RT2 resistance profiles are typified by aminoglycoside, phenicol, bicyclomycin, and, most significantly, multidrug resistance, with their corresponding microbiomes governed by a high abundance of *P. aeruginosa* and *K. pneumoniae*, both recognized organisms conferring high AMR and adverse clinical outcomes in bronchiectasis (34, 59, 60). Metagenomic assembly further confirmed *P. aeruginosa* as the top microbial taxon harboring the greatest amount of resistance genes, consistent with its high abundance within the RT2 cluster. Conversely, resistance gene distribution across other bacterial taxa highlights that macrolide, fluoroquinolone, β -lactam, and tetracycline resistance gene determinants, largely characteristic of RT1, are comparable to the previously described core airway resistome that is seen even in a nondiseased (healthy) state (10). Importantly, *R. mucilaginosa* has protective antiinflammatory properties, whereas *H. influenzae* and *Streptococcus* species link with improved bronchiectasis outcomes compared with *P. aeruginosa*, reflecting the microbial influences on the resistome of the RT1 and RT2 clusters, respectively (48, 61). It is assumed that antibiotic agent use would result in unfavorable changes to the resistome, but our data suggest this is not universally true. Remarkably, targeted *P. aeruginosa* eradication in chronically colonized individuals promoted a measurable shift from an unfavorable RT2 profile to an RT1 profile, suggesting the therapeutic potential of manipulating microbiomes in a targeted and specific manner to alter underlying resistomes (13). In contrast to pathogen-directed antimicrobial targeting, the BLESS (Bronchiectasis and Low-dose Erythromycin Study) trial underscores the importance of

indirect, nonbactericidal effects related to macrolide therapy, given the success of these agents in patients colonized by *P. aeruginosa*, an intrinsically macrolide-resistant pathogen. This further highlights the complex interplay between antibiotic therapy, the microbiome, and the resistome, whereby alternate mechanisms such as antiinflammatory effects and/or interference with bacterial quorum sensing further contribute to therapeutic response (13, 47). In line with our reported findings, successful *P. aeruginosa* eradication promoted reversion from an RT2 phenotype to an RT1 phenotype, highlighting distinct changes in microbiome and associated resistome profiles. Therefore, considering resistomes and subsequent targeted microbiome-directed therapy may prevent treatment failure, while acknowledging the broader impact of targeted therapies on the microbiome, including nonantibiotic effects. Notably, eradication therapy directed toward key pathogens like *P. aeruginosa* or *K. pneumoniae* may simultaneously reshape resistotypes, suggesting that bacterial load and resistance gene patterns are linked. This highlights that therapeutic strategies targeting specific pathogens can have broader implications on resistome dynamics beyond simply altering taxonomic abundance. Finally, we noted that several patients harboring *P. aeruginosa* in sputum culture exhibited RT1 resistotypes. This indicates that resistome profiles are not always defined by the presence of a single pathogen such as *P. aeruginosa* but may reflect a broader spectrum of complex microbial interactions and resistome dynamics.

Although novel, with several strengths, our work does have limitations. First, although we report the profiles of identified resistance genes in the airway, we do not make any inference about phenotypic resistance of the microbiome because this requires detailed functional *in vitro* experimentation. Although automated microbial genomic resistance prediction has been validated for specific pathogens (62), comprehensive standardization and validation of such predictions, pertaining to metagenomic analysis of the resistome, is yet to be achieved on comparable scales, and this remains a challenge. Although metagenomics has many advantages, it does have limitations, including the lack of detection of low-abundance resistance genes as a result of low coverage, which may, in practice, contribute to clinical resistance

and disease outcomes. Related to this, our metagenomic assembly approach, although it provided added novelty, is susceptible to “dropout” of lower-coverage genes and taxa that may be underrepresented. Although our experimental approach clearly provides important insight into the microbial origins of the resistome, the mobile nature of chromosomal resistance genes in association with mobile genetic elements must be considered, and the microbe–gene associations detected must therefore be interpreted cautiously (63). Our analysis did not include absolute quantification of resistance genes. Therefore, shifts in gene relative abundance may mask true levels of certain resistance genes (e.g., lower proportional representation of fluoroquinolone resistance genes in RT2), highlighting the interpretive limitations of metagenomic data when relying on relative abundance. Our short-read analytical pipeline for resistome characterization is dependent on the CARD ARG database, which, although comprehensive and internationally recognized, is not exhaustive and is capable of identifying only known resistance genes (30). This approach may be further biased by taxa that are well described and annotated in terms of their ARGs, which is undoubtedly the case for *P. aeruginosa* in the RT2 resistotype. Furthermore, the CARD “multi-drug” category is broad and includes genes that provide broad resistance to antibiotic agents including fluoroquinolones, even amid a lower detected abundance of typical fluoroquinolone resistance, as observed in the RT2 resistotype. Despite an appreciable trend of macrolide resistance (see Figure E2C), we failed to detect a significant effect of inhaled corticosteroids or long-term macrolide use on the resistome. However, we caution that our study was observational and therefore not specifically designed to test for systematic effects of therapy, which requires further analysis. It is also challenging to discern causation in terms of whether resistotype clusters precede the onset of disease activity, such as an exacerbation, or if patients with different disease endotypes undergo treatments that potentially lead to altered resistotypes. Geographic variations in bronchiectasis treatment across study sites, including preferred antibiotic agents, thresholds for antibiotic agent use, and criteria for treatment based on culture results or symptoms alone, may contribute to the observed resistome and microbiome

heterogeneity. Although a detailed analysis of these factors is beyond the scope of this study, we recognize them as potential limitations. In addition, our current knowledge of the airway “bacteriophage” remains limited, and, even though we did not identify clinical associations in this analysis, further work in this area may be warranted as greater airway metagenomic data become available. Finally, despite emerging evidence of the importance of a gut–lung axis in bronchiectasis, we did not investigate gut

microbiomes as a potential correlate of disease or reservoir for resistance (64). Given the profound impact of antibiotic agents on the gut microbiome, the inclusion of gut microbiome samples in future studies is warranted.

In conclusion, we describe the largest and most comprehensive assessment of the resistome in bronchiectasis to date, including its clinical relevance and translational potential. Our identification of novel resistotypes provides a fresh approach to

targeting the microbiome for therapeutic benefit, with potential application in patient care, antimicrobial stewardship, and clinical trial design. ■

Author disclosures are available with the text of this article at www.atsjournals.org.

Acknowledgment: The authors thank the Academic Respiratory Initiative for Pulmonary Health and the Lee Kong Chian School of Medicine Centre for Microbiome Medicine for collaboration support.

References

- Flume PA, Chalmers JD, Olivier KN. Advances in bronchiectasis: endotyping, genetics, microbiome, and disease heterogeneity. *Lancet* 2018;392:880–890.
- Mac Aogáin M, Chotirmall SH. Microbiology and the microbiome in bronchiectasis. *Clin Chest Med* 2022;43:23–34.
- Budden KF, Shukla SD, Rehman SF, Bowerman KL, Keely S, Hugenholtz P, et al. Functional effects of the microbiota in chronic respiratory disease. *Lancet Respir Med* 2019;7:907–920.
- Pailhoriès H, Herrmann JL, Velo-Suarez L, Lamoureux C, Beauruelle C, Burgel PR, et al. Antibiotic resistance in chronic respiratory diseases: from susceptibility testing to the resistome. *Eur Respir Rev* 2022;31:210259.
- Chotirmall SH, Chalmers JD. RESPIRE: breathing new life into bronchiectasis. *Eur Respir J* 2018;51:1702444.
- Haworth CS, Bilton D, Chalmers JD, Davis AM, Froehlich J, Gonda I, et al. Inhaled liposomal ciprofloxacin in patients with non-cystic fibrosis bronchiectasis and chronic lung infection with *Pseudomonas aeruginosa* (ORBIT-3 and ORBIT-4): two phase 3, randomised controlled trials. *Lancet Respir Med* 2019;7:213–226.
- De Soya A, Aksamit T, Bandel TJ, Criollo M, Elborn JS, Operschall E, et al. RESPIRE 1: a phase III placebo-controlled randomised trial of ciprofloxacin dry powder for inhalation in non-cystic fibrosis bronchiectasis. *Eur Respir J* 2018;51:1702052.
- Aksamit T, De Soya A, Bandel TJ, Criollo M, Elborn JS, Operschall E, et al. RESPIRE 2: a phase III placebo-controlled randomised trial of ciprofloxacin dry powder for inhalation in non-cystic fibrosis bronchiectasis. *Eur Respir J* 2018;51:1702053.
- Barker AF, O'Donnell AE, Flume P, Thompson PJ, Ruzi JD, de Gracia J, et al. Aztreonam for inhalation solution in patients with non-cystic fibrosis bronchiectasis (AIR-BX1 and AIR-BX2): two randomised double-blind, placebo-controlled phase 3 trials. *Lancet Respir Med* 2014;2:738–749.
- Mac Aogáin M, Lau KJX, Cai Z, Kumar Narayana J, Purbojati RW, Drautz-Moses DI, et al. Metagenomics reveals a core macrolide resistome related to microbiota in chronic respiratory disease. *Am J Respir Crit Care Med* 2020;202:433–447.
- Chotirmall SH, Dhar R, McShane PJ, Chang AB. Bronchiectasis: a global disease necessitating global solutions. *Lancet Respir Med* 2023;11:581–583.
- Chalmers JD, Haworth CS, Metersky ML, Loebeinger MR, Blasi F, Sibila O, et al.; WILLOW Investigators. Phase 2 trial of the DPP-1 inhibitor brensocatib in bronchiectasis. *N Engl J Med* 2020;383:2127–2137.
- Chotirmall SH, Bogaert D, Chalmers JD, Cox MJ, Hansbro PM, Huang YJ, et al. Therapeutic targeting of the respiratory microbiome. *Am J Respir Crit Care Med* 2022;206:535–544.
- Taylor SL, Leong LEX, Mobegi FM, Choo JM, Wesselingh S, Yang IA, et al. Long-term azithromycin reduces *Haemophilus influenzae* and increases antibiotic resistance in severe asthma. *Am J Respir Crit Care Med* 2019;200:309–317.
- Yi X, Li Y, Liu H, Liu X, Yang J, Gao J, et al. Inflammatory endotype-associated airway resistome in chronic obstructive pulmonary disease. *Microbiol Spectr* 2022;10:e0259321.
- Wang Z, Bafadhel M, Haldar K, Spivak A, Mayhew D, Miller BE, et al. Lung microbiome dynamics in COPD exacerbations. *Eur Respir J* 2016;47:1082–1092.
- Maurice CF, Haider HJ, Turnbaugh PJ. Xenobiotics shape the physiology and gene expression of the active human gut microbiome. *Cell* 2013;152:39–50.
- Noverr MC, Noggle RM, Toews GB, Huffnagle GB. Role of antibiotics and fungal microbiota in driving pulmonary allergic responses. *Infect Immun* 2004;72:4996–5003.
- Ivan FX, Mac Aogáin M, Jaggi TK, Keir HR, Dicker AJ, Lim AYH, et al. The Metagenomic ‘bacteriophage’ in bronchiectasis [abstract]. *Am J Respir Crit Care Med* 2021;203:A1216.
- Mac Aogáin M, Ivan FX, Jaggi T, Keir HR, Dicker AJ, Lim AYH, et al. The antimicrobial resistome in bronchiectasis: an international multicentre study [abstract]. *Eur Respir J* 2022;60(suppl 66):1559.
- Mac Aogáin M, Ivan FX, Jaggi T, Keir HR, Dicker AJ, Hou ALY, et al. The bronchiectasis ‘bacteriophage’. *Eur Respir J* 2021;58:OA1306.
- Pasteur MC, Bilton D, Hill AT; British Thoracic Society Bronchiectasis non-CF Guideline Group. British Thoracic Society guideline for non-CF bronchiectasis. *Thorax* 2010;65:i1–i58.
- Mac Aogáin M, Chandrasekaran R, Lim AYH, Low TB, Tan GL, Hassan T, et al. Immunological corollary of the pulmonary mycobiosis in bronchiectasis: the CAMEB study. *Eur Respir J* 2018;52:1800766.
- Bateman ED, Hurd SS, Barnes PJ, Bousquet J, Drazen JM, FitzGerald JM, et al. Global strategy for asthma management and prevention: GINA executive summary. *Eur Respir J* 2008;31:143–178.
- Vestbo J, Hurd SS, Agustí AG, Jones PW, Vogelmeier C, Anzueto A, et al. Global strategy for the diagnosis, management, and prevention of chronic obstructive pulmonary disease: GOLD executive summary. *Am J Respir Crit Care Med* 2013;187:347–365.
- Hill AT, Haworth CS, Aliberti S, Barker A, Blasi F, Boersma W, et al.; EMBARC/BRR definitions working group. Pulmonary exacerbation in adults with bronchiectasis: a consensus definition for clinical research. *Eur Respir J* 2017;49:1700051.
- Polverino E, Goeminne PC, McDonnell MJ, Aliberti S, Marshall SE, Loebeinger MR, et al. European Respiratory Society guidelines for the management of adult bronchiectasis. *Eur Respir J* 2017;50:1700629.
- Bolger AM, Lohse M, Usadel B. Trimmomatic: a flexible trimmer for Illumina sequence data. *Bioinformatics* 2014;30:2114–2120.
- Langmead B, Salzberg SL. Fast gapped-read alignment with Bowtie 2. *Nat Methods* 2012;9:357–359.
- Alcock BP, Raphenya AR, Lau TTY, Tsang KK, Bouchard M, Edalatmand A, et al. CARD 2020: antibiotic resistome surveillance with the comprehensive antibiotic resistance database. *Nucleic Acids Res* 2020;48:D517–D525.
- Kaminski J, Gibson MK, Franzosa EA, Segata N, Dantas G, Huttenhower C. High-specificity targeted functional profiling in microbial communities with ShortBRED. *PLOS Comput Biol* 2015;11:e1004557.
- Mac Aogáin M, Narayana JK, Tiew PY, Ali NABM, Yong VFL, Jaggi TK, et al. Integrative microbiomics in bronchiectasis exacerbations. *Nat Med* 2021;27:688–699.
- Segata N, Izard J, Waldron L, Gevers D, Miropolsky L, Garrett WS, et al. Metagenomic biomarker discovery and explanation. *Genome Biol* 2011;12:R60.

34. Dhar R, Singh S, Talwar D, Mohan M, Tripathi SK, Swarnakar R, *et al.* Bronchiectasis in India: results from the European Multicentre Bronchiectasis Audit and Research Collaboration (EMBARC) and Respiratory Research Network of India Registry. *Lancet Glob Health* 2019;7:e1269–e1279.
35. Chalmers JD, Polverino E, Crichton ML, Ringshausen FC, De Soyza A, Vendrell M, *et al.*; EMBARC Registry Investigators. Bronchiectasis in Europe: data on disease characteristics from the European Bronchiectasis registry (EMBARC). *Lancet Respir Med* 2023;11:637–649.
36. Li L, Mac Aogáin M, Xu T, Jaggi TK, Chan LLY, Qu J, *et al.* *Neisseria* species as pathobionts in bronchiectasis. *Cell Host Microbe* 2022;30:1311–1327.e8.
37. Mac Aogáin M, Tiew PY, Lim AYH, Low TB, Tan GL, Hassan T, *et al.* Distinct “immunoallotypes” of disease and high frequencies of sensitization in non-cystic fibrosis bronchiectasis. *Am J Respir Crit Care Med* 2019;199:842–853.
38. Chandrasekaran R, Mac Aogáin M, Chalmers JD, Elborn SJ, Chotirmall SH. Geographic variation in the aetiology, epidemiology and microbiology of bronchiectasis. *BMC Pulm Med* 2018;18:83.
39. Chalmers JD, Chang AB, Chotirmall SH, Dhar R, McShane PJ. Bronchiectasis. *Nat Rev Dis Primers* 2018;4:45.
40. Menzel P, Ng KL, Krogh A. Fast and sensitive taxonomic classification for metagenomics with Kaiju. *Nat Commun* 2016;7:11257.
41. Woo TE, Lim R, Heirali AA, Acosta N, Rabin HR, Mody CH, *et al.* A longitudinal characterization of the non-cystic fibrosis bronchiectasis airway microbiome. *Sci Rep* 2019;9:6871.
42. Cox MJ, Turek EM, Hennessy C, Mirza GK, James PL, Coleman M, *et al.* Longitudinal assessment of sputum microbiome by sequencing of the 16S rRNA gene in non-cystic fibrosis bronchiectasis patients. *PLoS One* 2017;12:e0170622.
43. Acosta N, Thomson CS, Surette MG, Somayaji R, Rossi L, Rabin HR, *et al.* Azithromycin and the microbiota of cystic fibrosis sputum. *BMC Microbiol* 2021;21:96.
44. Wang Y, Taylor SL, Choo JM, Papanicolaou LE, Keating R, Hindmarsh K, *et al.* Carriage and transmission of macrolide resistance genes in patients with chronic respiratory conditions and their close contacts. *Chest* 2022;162:56–65.
45. Chalmers JD, Aliberti S, Filonenko A, Shteinberg M, Goeminne PC, Hill AT, *et al.* Characterization of the “frequent exacerbator phenotype” in bronchiectasis. *Am J Respir Crit Care Med* 2018;197:1410–1420.
46. Metersky M, Chalmers J. Bronchiectasis insanity: doing the same thing over and over again and expecting different results? *F1000 Res* 2019;8:F1000.
47. Rogers GB, Bruce KD, Martin ML, Burr LD, Serisier DJ. The effect of long-term macrolide treatment on respiratory microbiota composition in non-cystic fibrosis bronchiectasis: an analysis from the randomised, double-blind, placebo-controlled BLESS trial. *Lancet Respir Med* 2014;2:988–996.
48. Dicker AJ, Loneragan M, Keir HR, Smith AH, Pollock J, Finch S, *et al.* The sputum microbiome and clinical outcomes in patients with bronchiectasis: a prospective observational study. *Lancet Respir Med* 2021;9:885–896.
49. Keir HR, Shoemark A, Dicker AJ, Perea L, Pollock J, Giam YH, *et al.* Neutrophil extracellular traps, disease severity, and antibiotic response in bronchiectasis: an international, observational, multicohort study. *Lancet Respir Med* 2021;9:873–884.
50. Chotirmall SH, Chalmers JD. Bronchiectasis: an emerging global epidemic. *BMC Pulm Med* 2018;18:76.
51. Chotirmall SH, McShane PJ. Time to acknowledge, address, and take action against bronchiectasis. *Lancet Glob Health* 2019;7:e1162–e1163.
52. Mac Aogáin M, Jaggi TK, Chotirmall SH. The airway microbiome: present and future applications. *Arch Bronconeumol* 2022;58:8–10.
53. Lee H, Choi H, Chalmers JD, Dhar R, Nguyen TQ, Visser SK, *et al.* Characteristics of bronchiectasis in Korea: first data from the Korean Multicentre Bronchiectasis Audit and Research Collaboration registry and comparison with other international registries. *Respirology* 2021;26:619–621.
54. Visser SK, Bye PTP, Fox GJ, Burr LD, Chang AB, Holmes-Liew CL, *et al.* Australian adults with bronchiectasis: the first report from the Australian Bronchiectasis Registry. *Respir Med* 2019;155:97–103.
55. Aksamit TR, O'Donnell AE, Barker A, Olivier KN, Winthrop KL, Daniels MLA, *et al.*; Bronchiectasis Research Registry Consortium. Adult patients with bronchiectasis: a first look at the US Bronchiectasis Research Registry. *Chest* 2017;151:982–992.
56. Dhar R, Singh S, Talwar D, Murali Mohan BV, Tripathi SK, Swarnakar R, *et al.*; EMBARC-India study group. Clinical outcomes of bronchiectasis in India: data from the EMBARC/Respiratory Research Network of India registry. *Eur Respir J* 2023;61:2200611.
57. Ali NABM, Ivan FX, Mac Aogáin M, Narayana JK, Lee SY, Lim CL, *et al.* The healthy airway mycobioime in individuals of Asian descent. *Chest* 2021;159:544–548.
58. Lee SY, Mac Aogáin M, Fam KD, Chia KL, Binte Mohamed Ali NA, Yap MMC, *et al.* Airway microbiome composition correlates with lung function and arterial stiffness in an age-dependent manner. *PLoS One* 2019;14:e0225636.
59. Finch S, McDonnell MJ, Abo-Leyah H, Aliberti S, Chalmers JD. A comprehensive analysis of the impact of *Pseudomonas aeruginosa* colonization on prognosis in adult bronchiectasis. *Ann Am Thorac Soc* 2015;12:1602–1611.
60. Guiton AK, Wright GD. Antimicrobial resistance and respiratory infections. *Chest* 2018;154:1202–1212.
61. Rigauts C, Aizawa J, Taylor SL, Rogers GB, Govaerts M, Cos P, *et al.* *Rothia mucilaginosa* is an anti-inflammatory bacterium in the respiratory tract of patients with chronic lung disease. *Eur Respir J* 2022;59:2101293.
62. Bradley P, Gordon NC, Walker TM, Dunn L, Heys S, Huang B, *et al.* Rapid antibiotic-resistance predictions from genome sequence data for *Staphylococcus aureus* and *Mycobacterium tuberculosis*. *Nat Commun* 2015;6:10063.
63. Lv L, Wan M, Wang C, Gao X, Yang Q, Partridge SR, *et al.* Emergence of a plasmid-encoded resistance-nodulation-division efflux pump conferring resistance to multiple drugs, including tigecycline, in *Klebsiella pneumoniae*. *mBio* 2020;11:e02930-19.
64. Narayana JK, Aliberti S, Mac Aogáin M, Jaggi TK, Ali NABM, Ivan FX, *et al.* Microbial dysregulation of the gut-lung axis in bronchiectasis. *Am J Respir Crit Care Med* 2022;207:908–920.